Title

Caspase-6-cleaved tau is relevant in Alzheimer's disease but not in 4-repeat tauopathies: diagnostic and therapeutic implications

Authors

Panos Theofilas[1, 8], Antonia M.H. Piergies[1, 8], Song Hua Li[1], Cathrine Petersen[1], Alexander J. Ehrenberg[1], Rana A. Eser[1], Brian Chin[2], Teddy Yang[2], Shireen Khan[3], Raymond Ng[3], Salvatore Spina[1], Willian W. Seeley[1, 4], Bruce L. Miller[1, 5], Michelle R. Arkin[6, 9 *], and Lea T. Grinberg[1, 4, 5, 7, 9 *]

(1) Memory and Aging Center, UCSF Weill Institute for Neurosciences, University of California, San Francisco, San Francisco, CA, USA

(2) Shanghai ChemPartner, Shanghai, China

(3) ChemPartner San Francisco, South San Francisco, CA, USA

(4) Department of Pathology, University of California, San Francisco, San Francisco, CA, USA

(5) Global Brain Health Institute, University of California, San Francisco, San Francisco, CA, USA

(6) Department of Pharmaceutical Chemistry and Small Molecule Discovery Center, UCSF, San Francisco, CA, USA

(7) Department of Pathology, University of Sao Paulo Medical School, Sao Paulo, Brazil

(8) Co-first author

(9) Co-senior author

***Correspondence**

1. Lea T. Grinberg, MD, PhD; John Douglas French Alzheimer's Foundation Endowed Professor; Associate Professor of Neurology and Pathology; University of California, San Francisco; 675 Nelson Rising Lane, 211B, Box 1207; San Francisco, CA 94158; Email: lea.grinberg@ucsf.edu; Phone: (415) 502-7229

2. Michelle R. Arkin, PhD; Thomas William and Frederick John MacWilliam Distinguished Professor of Pharmaceutical Chemistry; co-Director, Small Molecule Discovery Center; School of Pharmacy, University of California San Francisco; Box 2552; 1700 4th Street. San Francisco, CA. 94143; Email: Michelle.arkin@ucsf.edu; Phone: (415) 514-4313

Abstract

Aim

Tau truncation (tr-tau) by active caspase-6 (aCasp-6) generates toxic tau fragments prone to self-aggregation. Yet, the relationship between aCasp-6, different forms of tr-tau, and hyperphosphorylated tau (p-tau) accumulation in human brains with Alzheimer's disease (AD) and other tauopathies remains unclear.

Methods

We generated two neoepitope monoclonal antibodies against tr-tau sites (D402 and D13) targeted by aCasp-6. Then, we used 5-plex immunofluorescence to quantify the neuronal and astroglial burden of aCasp-6, tr-tau, p-tau, and their co-occurrence in healthy controls, AD, and primary tauopathies.

Results

Casp-6 activation was strong in AD, followed by Pick's disease (PiD), but almost absent in 4-repeat (4R) tauopathies. Tr-tau neuronal burden was much higher in AD than in 4R tauopathies, and disproportionally higher when normalizing by p-tau pathology. Tr-tau astrogliopathy was detected in low numbers in 4R tauopathies. Unexpectedly, half of the tr-tau positive neurons in AD lacked p-tau aggregates.

Conclusions

Early modulation of aCasp-6 with consequent amortization of tr-tau pathology is a promising therapeutic strategy in AD and possibly PiD, but it is unlikely to benefit 4R tauopathies. The large percentage of tr-tau neurons lacking p-tau suggests that not all tau pathology and vulnerable neurons are detected by conventional p-tau Ser 202 antibody and, that AD, has distinct mechanisms of tangle formation. Therapeutic strategies against tr-tau pathology could modulate tau abnormalities in AD. The disproportional higher burden of tr-tau in AD supports the evaluation of biofluid biomarkers against N-terminus tr-tau to detect AD and differentiate it from 4R tauopathies at a single patient level.

Keywords

Alzheimer's disease, tauopathies, tau cleavage, tau hyperphosphorylation, tau isoforms, caspase-6, cell counting, immunohistochemistry.

Abbreviations

3R 3-repeat
4R 4-repeat
aCasp-6 active caspase-6
AD Alzheimer's disease
AGD Argyrophilic grain disease
CBD Corticobasal degeneration
IF Immunofluorescence
ITG inferior temporal gyrus
MFG middle frontal gyrus
mAb monoclonal antibody
NFT Neurofibrillary tangle
p-tau Hyperphosphorylated tau
PHF Paired helical filaments
PiD Pick's disease
PSP Progressive supranuclear palsy
PTM Post-translational modifications
tr-tau Truncated tau
TMA Tissue microarrays

Introduction

Tau post-translational modifications (PTMs) define and modulate tau function in healthy and diseased states. Tauopathies, a major group of neurodegenerative diseases [1–3] including Alzheimer's disease (AD), Pick's disease (PiD), corticobasal degeneration (CBD), progressive supranuclear palsy (PSP), and argyrophilic grain disease (AGD), share a progressive accumulation of pathological tau in the brain. Although tauopathies are classically defined by the morphology and distribution of phosphorylated tau (p-tau) aggregates, other underexplored tau PTMs are also critical to tau pathogenesis [4–6].
Proteolytic truncation of tau (tr-tau) by active caspases has been recently recognized as a significant contributor to tau-driven nosology in AD and primary tauopathies [7–10]. Caspases - cysteine-aspartic proteases - are proteolytic enzymes with well-defined roles in apoptosis and inflammation [11, 12]. Pro-apoptotic caspase-6 is an effector caspase, along with caspases-3 and -7. Due to the central role of caspase-3 in stress-induced apoptosis and neuronal death in development, most studies are directed at this caspase. Nevertheless, previous studies, including ours, demonstrate high levels of active caspase-6 (aCasp-6) and not -3 in the AD brain that co-occurs with an increase of abnormal proteins associated with the disease, including the amyloid precursor protein and phospho-tau [13–16]. Caspase-6 promotes apoptosis downstream [12, 17, 18]. Besides, caspase-6 acts upstream in AD, by cleaving tau at confirmed and putative sites, including tau cleavage at Asp421, a C-terminus site (D421) contributing to tau aggregation and the formation of tau neurofibrillary tangles (NFTs) [7, 9, 19].

We previously detected an increasing burden of neurons with aCasp-6 in AD starting at initial stages that paralleled the increasing burden of phospho-tau (p-tau) Ser 202 in neurons, with co-occurring aggregates [16]. This early and progressive increase of aCasp-6levels in AD corroborates the hypothesis that modulation of caspase-6 activation and cleavage of tau may represent a promising therapeutic strategy in AD. However, fundamental gaps in our understanding of caspase-6 activation and tau cleavage and the relationship between these processes and the formation of p-tau aggregates in neurons and glia persist. For example, it is unclear whether aCasp-6 is detected in tauopathies other than AD and the knowledge about the burden of tr-tau forms or to which extent these tr-tau and p-tau aggregates co-occur in the same cells is practically limited to D421 in AD among all tauopathies. Moreover, D421 is not the only tr-tau form to accumulate in AD. Caspase-6 targets tau at other sites in AD, including D402 at the C-terminus and D13 at the N-terminus [14, 20, 21]. In AD, D402 levels in NFTs and neuropil threads are associated with lower global cognitive scores in cases with no cognitive impairment, indicating that tau truncation may be an early event in AD pathogenesis [13]. Levels of D402 (detected by polyclonal antibodies) correlates with pathological p-tau and neuronal loss in human brains affected by AD and has been tested as a CSF biomarker for AD since its levels positively correlate with AD severity [14, 20, 22]. Moreover, in vitro studies have shown that tau cleavage by caspase-6 at D13, which is at the center of the Tau-12 and 5A6 epitopes, results in the loss of immunoreactivity with both Tau-12 and 5A6 N-terminal antibodies, suggesting a role for caspase-6 in the N-terminal truncation of tau [21]. However,

investigation on D13 and D402 truncated forms have been limited by the lack of reliable monoclonal antibodies targeting these specific cleavage sites.

To interrogate the spread of caspase-6 tr-tau in human tauopathies and the potential relevance of therapeutic modulation of caspase-6 activity in these diseases, we generated two monoclonal neoepitope antibodies (mAbs) against proteolytic sites predominantly targeted by caspase-6: D402 and D13. Next, we used multiplex immunofluorescence (IF) to quantitatively map neurons and glia with D402 and D13 tr-tau and evaluate their relationship to p-tau Ser 202 aggregates and aCasp-6 in two cortical areas of a well-characterized postmortem brain cohort with AD, sporadic 3-repeat (3R), and 4-repeat (4R) tauopathies and healthy aging controls.

Materials and Methods

Participants

This study was exempt from ethical approval by the University of California, San Francisco (UCSF) institutional review board. Postmortem human brains were obtained from UCSF's Neurodegenerative Disease Brain Bank [23]. All brains underwent standardized neuropathological assessment for neurodegenerative diseases that follow universally accepted guidelines [24, 25]. Inclusion criteria included a postmortem interval under 24 hours and a lack of more than one neuropathological diagnosis, an Axis I psychiatric disorder diagnosis, a non-dementia neurological disorder, or gross non-degenerative structural neuropathology. Control cases were free of any clinical symptoms of cognitive decline and neurological or non-incidental neuropathological diagnoses. To provide a broad picture of the most common sporadic tauopathies, our cohort of cases include 3R and 4R tauopathies–AD (3R/4R), AGD (4R), CBD (4R), PiD (3R), PSP (4R)–as well as clinically and pathological age-matched controls. Table 1 illustrates the characteristics of all 17 cases.

Development of caspase-6-cleaved tau neoepitope monoclonal antibodies

Except for TauC3 (D421), mAbs against caspase-6 tr-tau were not available. In collaboration with ChemPartner, we generated two neoepitope mAbs against tr-tau by caspase-6: mAbD13 (14-442; Peptide I: HAGTYGLGDRKC) and mAbD402 (1-401; Peptide II: CIVYKSPVVSGD) as previously described [26]. Briefly, both mAbs were produced by immunizing 6- to 8-week-old wild type Balb/c, and SJL mice (SLAC) with keyhole limpet hemocyanin (KLH) conjugated tau peptides using protocols approved by the ChemPartner IACUC committee. 50 µg of each peptide was injected into each mouse's abdominal cavity along with 0.25 mL of Complete Freund's Adjuvant (Sigma). Blood samples were collected one week after immunization. The antibody titer and specificity in serum were determined by enzyme-linked immunosorbent assay (ELISA) analysis against BSA-conjugated peptides I and II, and western blot against full-length tau, tau 1-402, and tau 14-441 recombinant proteins. Mice with specific immune responses against tau peptides were selected for fusion and were given a final boost by intraperitoneal injection of 100 µg of the corresponding immunogen. After four days, all mice were sacrificed, and their splenocytes lysed in NH4OH at 1% (w/w), followed by centrifugation at 1000 rpm and washes with DMEM (Invitrogen). Viable splenocytes were fused with mouse

myeloma cells SP2/0 (ATCC) at a ratio of 5:1 with high-efficiency electric fusion (BTX ECM200). Fused cells were re-suspended in DMEM with 20% FBS and hypoxanthine-aminopterin-thymidine (HAT) medium (Invitrogen). 14 days after cell fusion, hybridoma supernatants were collected and screened by ELISA. Clones with an OD450 nm > 1.0 were expanded in a 24-well plate containing DMEM with 10% heat-inactivated FBS, and supernatants were collected after three days of culture. The antibody isotypes were determined, and ELISA and western blot were used to test their ability to bind to tau. Clones that showed desired reactivity and specificity against tau were subjected to subcloning to get stable monoclonal hybridoma cells. Sub-cloning was carried out by limited dilution in a 96-well plate with DMEM media containing 10% FBS. Clones with specific tau binding were further expanded in DMEM media containing 10% FBS for subsequent antibody production and cryopreservation. See Supplemental Experimental Procedures for the analysis of antibody specificity.

Tissue processing and multiplex immunofluorescence staining

Immunofluorescence (IF) assays are prone to batch variations. To minimize this risk, we created tissue microarrays (TMAs) by using a 5 mm biopsy punch to sample the middle frontal gyrus (MFG) at the level of the optical chiasm and the inferior temporal gyrus (ITG) at the level of anterior commissure from all 17 cases. The longest punch axis was always perpendicular to the gyrus surface to avoid oblique sampling. Each TMA accommodated six cases that were embedded in a single paraffin block. Eight µm thick sections of each TMA were mounted on histological slides before undergoing multiplex IF, through which we would detect neurons (NeuN), p-tau (CP13), aCasp-6, and caspase-6 tr-tau (see Table S1 for a list of primary antibodies). We chose CP13 as a proxy for p-tau because phosphorylation of tau at Ser 202 occurs earlier in AD, is present in all tauopathies, and rarely occurs in healthy brains [27–30]. All IF assays were performed using a Ventana Discovery Ultra automated staining instrument (Ventana Medical Systems). The general procedure and quality control steps of our IF protocol have been described in detail elsewhere [31]. Briefly, tissue sections were baked at 60°C for 20 minutes and subsequently deparaffinized via incubation in 69°C Ventana's Discovery wash solution for 24 minutes. Epitope retrieval was accomplished by incubating sections in a 95°C Discovery CC1 solution (Ventana) for 56 minutes. Following epitope retrieval, sections were incubated in room temperature Discovery inhibitor (Ventana) for 16 minutes to inactivate endogenous horseradish peroxidase (HRP). See Supplemental Experimental Procedures for antibody labeling approach.

Quantitative analysis of positive markers

Cell quantification was performed blinded to clinical and neuropathological diagnosis. Three independent evaluators performed quantification. Each tissue punch was imaged at 20x magnification with a Zeiss AxioImager A2 microscope equipped with a Zeiss Colibri 7: Type FRR [G/Y] CBV-UC 7-channel fluorescence light source and an electronic platform. AF350 was visualized using a DAPI filter set, AF488 with a GFP filter set, AF546 with a DsRed filter set, AF647 with a Cy5 filter set, and AF790 with a Cy7 filter set. Figures 1 and 2 show representative examples of positive markers in neurons (all tauopathies) and astroglia (PSP and CBD),

respectively. A semi-automated pipeline was used to quantify marker positivity in both cell types (Figure 3). The quantitative approach is described in Supplemental Experimental Procedures.

Statistical analysis

Data analysis was performed using R Statistical Software (version 3.6.1; R Foundation for Statistical Computing, Vienna, Austria). Means and standard deviations were calculated for demographic and quantitative neuropathological data.

Results

Table 1 summarizes the demographic, clinical, and neuropathological characteristics of all 17 cases used in this study. 52.94% were male, the mean (SD) age of death was 70.82 (9.29) years, the mean (SD) postmortem interval was 10.18 (3.96) hours, and the mean (SD) brain weight was 1148.94 (124.79) grams.

All tauopathies show expected positivity for neuronal p-tau

We used the p-tau mAb CP13 (Table S1) to map p-tau Ser 202-positive neurons in five sporadic tauopathies and healthy controls. All cases showed the expected percentages and distributions of neuronal p-tau inclusions in the MFG and ITG. In the MFG, the absence of neuronal p-tau in AGD was anticipated since this region is typically spared of tau pathology. Of note, in controls, we found p-tau positivity in an average of 0.09% of ITG neurons, within the bounds expected of non-pathological aging. Overall, our results confirm the presence of tau lesions in predicted regions based on disease diagnosis and provide a basis for us to interpret the magnitude of tr-tau burden (Table 2; Figures 4, 5).

The percentage of neurons positive for active caspase-6 in AD is at least 2.11 times higher than in all other tauopathies tested

In AD, aCasp-6 promotes tau cleavage. We previously found that the percentage of neurons with aCasp-6 increases as the disease progresses [16]. Here, we asked if this increase is a feature of other common tauopathies (Table 2; Figures 4, 5). In AD, we detected an average of 8.74% neurons in MFG neurons and 8.79% neurons in ITG positive for aCasp-6. In control cases, we did not find any aCasp-6 positivity in either region. The percentage of MFG and ITG neurons with aCasp-6 positivity in AD was much higher than that in all other tauopathies tested. PiD, the tauopathy with the second-highest number of neurons with aCasp-6 positivity, only had aCasp-6 in 4.15% of MFG neurons and 1.26% of ITG neurons. These findings demonstrate that neuronal caspase-6 activity seems to be strongest in AD, moderate in PiD, and negligible in other tauopathies, pointing to potential differences in caspase-dependent tau-cleavage, and thus therapeutic approaches in AD and non-AD tau.

Neuronal caspase-6-cleaved tau aggregates are prominent in AD and PiD but not in 4-repeat tauopathies

Previous studies focusing on the tr-tau sites D421 (mAbTauC3) and D402 (polyclonal antibody) showed tr-tau aggregates in AD, but relatively little is known about tr-tau aggregates in common primary tauopathies. Here, we used novel neoepitope mAbs targeting caspase-6 tr-tau at a C-terminus site (D402) and a previously not directly explored N-terminus site (D13) to quantify the magnitude of tr-tau pathology in AD and other tauopathies (Figures 4, 5). Overall, AD and PiD exhibited at least 1.80x neuronal positivity for mAbD402 than the other tauopathies, reaching as much as 8.67% in MFG neurons and 7.08% ITG neurons in AD. Percentages were similar for mAbD13 (8.63% of MFG neurons and 8.03% of ITG neurons). Although the proportion of D13 tr-tau neurons was noteworthy in PiD, with positivity in 5.61% of MFG neurons and 3.30% of ITG neurons, D402 tr-tau was less abundant (only 0.97% of MFG and 0.98% of ITG neurons). All other diseases showed minimal percentages (≤1%) of neurons with mAbD402 or mAbD13 positivity (Table 2; Figures 4, 5). These results suggest that caspase-6-cleaved tau is a more defining feature of tauopathies with 3R tau aggregates (AD and PiD) than 4R tau aggregates (AGD, CBD, and PSP). Also, it highlights the potential of measuring D402 levels as a potential fluid-based biomarker to differentiate AD from other tauopathies

In AD, the tauopathy with the highest percentage of active caspase-6 positive neurons, 89.6% of these neurons also harbor tr-tau. Co-occurrence was lower in the opposite direction, as only 72.70-76.45% (mAbD402) and 65.44-84.38% (mAbD13) of tr-tau neurons were also positive for aCasp-6 in AD. Intriguingly, in PiD, only about 1/3 of tr-tau positive neurons were also positive for aCasp-6 (Table 2; Figures 4, 5).

In AD, a substantial percentage of neurons with tr-tau lack p-tau Ser 202 inclusions.

P-tau inclusions are the hallmark of all tauopathies, and the abnormal tau-phosphorylation at Ser202 is considered one of the earliest and universal events in tau pathogenesis. Here, we evaluated the degree of co-occurrence between p-tau and tr-tau at D402 and D13 cleavage sites (Table 2; Figures 4, 5). Since the number of neurons with D402 and D13 tr-tau were minimal in the tested 4R tauopathies (PSP, CBD, and AGD), we focused on AD and PiD. Concerning the co-occurrence of tr-tau and p-tau, in PiD, 80.65 and 76.30% of MFG neurons with D402 and D13 tr-tau, respectively, also showed p-tau. Percentages were similar in ITG neurons (81.82% and 87.67%). Surprisingly, in AD, only 32.81 and 52.59% of MFG neurons and 26.30% and 64.22% of ITG neurons with D402 and D13 tr-tau inclusions showed p-tau Ser202 positivity These results were unexpected and suggested a significant population of neurons harboring abnormal tau changes that would not be captured in studies only focusing on p-tau and are thus neglected investigations related to selective vulnerability and pathogenesis of AD and a lesser extent, PiD. Interestingly, D402 and D13 tr-tau species only show partial neuronal co-occurrence in AD (Table 2; Figures 4, 6).

Glial caspase-6-cleaved tau inclusions in PSP and CBD.

Tau deposits in astroglia are a prominent feature of PSP and CBD [32]. Previous studies suggest D421 tr-tau glial pathology [8], but it less clear if D13 and D402 tr-tau also accumulate in astroglia. Here, we focused on p-

tau (Ser202)-positive glia in PSP and CBD since these tauopathies show dominant tau lesions in glia. We used the same tissue sections to quantify neuronal tau pathological changes and tr-tau D402 and D13 mAbs. PSP showed strong p-tau positivity in tufted and thorned astrocytes in the MFG and ITG (Table S2; Figures 2, 6). In CBD, p-tau positivity in astrocytic plaques was also strong. In the MFG, likewise of what was observed in neurons, only a small percentage of p-tau -positive astrocytes (8.99%), also showed caspase-6 activity in PSP, and even less in CBD (3.70%). Overall, the percentage of p-tau positive glia with overlapping tr-tau was higher in PSP than in CBD, and D13 was more prevalent than D402 tr-tau in both brain regions (Table S2). We failed to observe astroglia with tr-tau inclusion lacking p-tau. Our results suggest that astroglia also show caspase-6 tr-tau species at novel D13 and D402 sites. However, the percentage is small, and tr-tau is practically absent in astrocytic plaques in CBD, reinforcing the observation that tr-tau pathology is much more prominent in tauopathies with abnormal 3R tau deposits.

Discussion

We developed a 5-plex immunofluorescence (IF) protocol [31], with novel monoclonal antibodies (mAbs) recognizing caspase cleavage sites on tau, and quantitative analyses in tissue microarray (TMA) blocks containing well-characterized postmortem brain tissue from two cortical areas of common tauopathies and healthy controls to investigate the following questions: 1) Is there evidence of aCasp-6 in non-AD tauopathies? 2) Besides D421, is the accumulation of caspase-6 tr-tau fragments present in AD and other tauopathies? 3) What is the pattern of co-occurrence of N- and C-terminus tr-tau fragments, p-tau, and aCasp-6 within the same neurons? 4) Do neurons with tr-tau inclusions also show evidence of p-tau? and 5) Are aCasp-6 and tr-tau inclusions also present in p-tau positive astroglia in PSP and CBD? This study offers several novel findings informing on mechanisms, diagnostic, and therapeutic strategies in AD and other tauopathies.

First, both amounts of caspase-6 activation and neuronal tr-tau burden were much higher in AD and to a lesser extend in PiD than in 4R tauopathies. In fact, evidence of caspase-6 activation was almost absent in pure 4R tauopathies (Table 2 and S2 and Figures 4, 6). aCasp-6 mediates truncation of tau in toxic tau fragments prone to self-aggregation [7, 9, 19] thus it is not surprising that compared to the 4R tauopathies, the mean percentages of neurons with D402 and/or D13 tr-tau were between 9.2-fold (D402 compared to PSP in MFG) to 236-fold higher in AD (D402 compared to CBD in ITG) and up to 32.67-fold higher in PiD. In a recent investigation, we showed that caspase-6 inhibitors rescue tau pathology in iPSC-derived neurons with the V337M MAPT mutation [16]. Caspase inhibitors are a promising therapy for tauopathies with 3R tau or mixed 3R/4R pathological forms but are unlikely useful for 4R tauopathies.

Second, the higher tr-tau burden in AD compared to other tauopathies was greater than expected based on the burden of p-tau Ser 202 inclusions. This result is also true, though to a lesser extent, in PiD. The percentage of p-tau neurons in AD was only 5x (PSP in MFG vs 9.2x for tr-tau) or 3.2x (CBD in ITG vs 236x for tr-tau) greater. The disproportional higher burden of tr-tau than p-tau in AD relative to 4R tauopathies suggests that

biofluid biomarkers based on tr-tau may be superior to p-tau biomarkers to diagnose AD and differentiate it from other tauopathies [33]. Developing biofluid-based biomarkers to detect D13 tr-tau is attractive and feasible. CSF is depleted of C-terminal tau peptides, making it challenging to detect fragments above residue 268, including D421 [34, 35]. Our multiplex IF approach enabled us to establish that N-terminus tr-tau (D13) is more abundant in neurons relative to the C-terminus form (D402), though they exhibit a high degree of co-occurrence. Recent studies on biofluid-biomarkers with N-terminal assay (NT1), which includes the N-terminal mAbTau12 (amino acids 6–13), show that the higher the NT1 levels, the worse the clinical decline in subjects with positivity for other AD biomarkers. NT1 levels remain intact in cases classified as non-AD dementia [36–38]. Corroborated by our quantitative neuropathological results and success of other N-terminal truncated assays, mAbD13 may become an essential player in the arsenal of biofluid biomarkers against AD.

Third, intriguingly, in AD approximately half of the neurons with tr-tau inclusions do not also stain positive for p-tau (Ser 202). The significant number of tr-tau-only cells may be highly relevant for understanding AD pathology, since neurons accumulating tr-tau may follow a pathogenic pathway independent of tau phosphorylation. Furthermore, most pathology centers rely on detecting and mapping p-tau (Ser 202) inclusions for classifying and staging tauopathies in humans and experimental models. Thus, a set of neurons with pathological tau has been systematic excluded from investigations focusing on AD pathogenesis and determinants of selective neuronal vulnerability. Our findings seem to disagree with a previous study suggesting that tau phosphorylation precedes tau truncation in AD [8] and it is possible that these neurons have lost p-Ser202 signal along the disease progression. However, experimental and postmortem human studies support our findings by demonstrating that tr-tau is an early event leading to filament formation in tauopathies [9, 19, 39–41]. For instance, Horowitz et al. detected N-terminal tau truncation, preceding C-terminal truncation and phosphorylation at p-tau th18 in AD [21]. Regarding tau pathogenesis, our study supports the notion that therapeutic approaches for modulating the generation of tr-tau species, including the use of caspase-6 inhibitors or mAbD13, may effectively treat AD in addition to strategies aimed to modulate the accumulation of p-tau species.

Forth, although most neurons with aCasp-6 also harbor tr-tau inclusions, the opposite is not necessarily true. In AD, almost 9/10 neurons with aCasp-6 also harbor tr-tau inclusions, while 3/4 of tr-tau inclusions show evidence of aCasp-6. The difference could be attributed to the ephemeral nature of caspase activity compared to tau truncation [7]. Thus, the latter at more likely to be detected in a cross-sectional study. However, findings in PiD suggest that additional explanations may be needed since only about 1/3 of tr-tau neurons showed evidence of aCasp-6. Perhaps caspase-6 activation is even more ephemeral in PiD than AD, or other caspases, such as caspase-2, 3, 7, or 8 may cleave tau at the D402 and D13 sites. To address this possibility, we performed immunostaining in AD tissue using antibodies against caspase-3, but found no positivity (data are not shown), in line with other studies failing to identify caspase-3 activation [14, 42, 43]. Further studies testing caspase-2, -7 and -8 activity in tauopathies are warranted.

Finally, small numbers tr-tau (D13) and, to a lesser extent, tr-tau (D402) are also present in p-tau positive glia in PSP. Tr-tau is also observed to a small extent in CBD. Thus, caspase-mediated tau pathological changes extend beyond neurons in tauopathies (Figure 6, Table S2), in line with previous findings using the mAbTauC3 (D421) [8].

Our approach includes measures to maximize analytical rigor. Multiplex IF methods have been limited by difficulties in eluting any antibody, including tau antibodies while maintaining tissue integrity to allow multiple staining cycles in the same histological slide. Here, we applied a pipeline recently developed in-house that provides excellent elution of tau antibodies verified by rigorous quality control steps [31]. Our methodology enabled us to examine three tau antibodies raised against the same species simultaneously. Also, the simultaneous use of several antibodies in the same tissue section increases the confidence of our results. To avoid bias in the quantification due to immunostaining batch variation, we produced TMAs containing multiple brain specimens in each single paraffin block. This approach also minimizes the chances of false-negative results. For instance, all our tissue samples, except for AGD which is not expected to show p-tau positivity in the MFG [44, 45], showed strong p-tau positivity, and whereas CBD almost lacked evidence of caspase-6 activation compared to the other punches in the same TMA (Table 2; Figures 4, 5). TMA is a common approach in cancer research but still developing in neurodegenerative diseases. Also, we quantified neurons and pathological inclusions in two separate sets of slides of the case cases, with similar results. Nevertheless, our approach is not free of limitations. Many of them are inherent to postmortem studies in the human brain, including the cross-sectional nature and the relatively small number of cases analyzed. Obtaining well-characterized postmortem human brain tissue from healthy controls and rare tauopathies, especially those from cases lacking neuropathological comorbidities, is challenging. Despite its relatively small size, we counted over 40,000 individual neurons in MFG and ITG combined.

In summary, this study uses two new tr-tau antibodies to demonstrate a strong association between aCasp-6 and truncated tau and suggests that caspase-6 cleavage of tau in neurons is likely a feature of tauopathies with 3R tau rather than 4R tau. Our results highlight the importance of studies comparing different tauopathies side-by-side as their similarities and differences may inform the pathogenesis. Furthermore, a significant percentage of tr-tau neurons in AD lacked evidence of p-tau. Considering the progressive nature of AD and other tauopathies, early modulation of caspase-6 activation and caspase cleavage of tau could have a significant therapeutic value against tau aggregation and neuronal death. This study further supports the potential of biofluid biomarkers for detecting tr-tau forms to diagnosing AD and differentiating AD from other tauopathies at the single patient level. Further studies in the human brain and clinically-relevant models of tau pathology, such as iPSCs from patients with MAPT mutations [46], are crucial for better understanding caspase-mediated pathways that lead to tau pathology in tauopathies.

Author Contributions

P.T., A.M.H.P., and L.T.G. designed the study; P.T. and A.M.H.P., performed the experiments, data acquisition, and analyses. B.C.,T.Y., S.K., R.N., and M.R.A. generated the neoepitope caspase-cleaved tau antibodies. S.L, A.J.E, and R.A.E contributed to immunohistochemistry and C.P. with data analyses and graphic design. S.S, W.W.S., B.L.M, and L.T.G provided the human brain specimens, P.T. and A.M.H.P. wrote the manuscript, S.S, W.W.S., B.L.M, M.R.A., and L.T.G. revised the manuscript, L.T.G. supervised the study and approved the submitted version.

Acknowledgments

We thank the patients and their families for their invaluable contribution to brain aging neurodegenerative disease research. We thank Dr. Andrea LeBlanc for helpful discussions on caspase biochemistry and Dr. Peter Davies (Albert Einstein College of Medicine, New York, NY) for generously providing tau antibodies. This study was supported by the National Institutes of Health K01AG053433 (P.T), K24AG053435, R56AG057528 and U54 NS100717 (L.T.G), K08AG052648 (S.S), P30AG062422 and P01AG019724 (B.L.M), UCSF RAP Pilot Award program (P.T), UCSF RAP Team Science Grant (L.T.G., M.R.A.), Alzheimer's Association AARG-16-441514 (L.T.G., M.R.A.), Rainwater Charitable Foundation (M.R.A.), and a Catalyst award from ShangPharma Innovation (M.R.A., T.Y., S.K, R.N.).

Ethical approval

The use of human brain tissue has received ethical approval by the University of California San Francisco Institutional Review Board.

Conflict of interest

M.R.A. is cofounder of Elgia Therapeutics, which is developing caspase-6 inhibitors for inflammatory diseases. The other authors have declared no conflict of interest.

Data Availability Statement

The data that support the findings of this study are available from the corresponding author upon reasonable request.

References

1. Spillantini MG, Goedert M (2013) Tau pathology and neurodegeneration. Lancet Neurol 12:609–622

2. Rösler TW, Tayaranian Marvian A, Brendel M, et al (2019) Four-repeat tauopathies. Prog Neurobiol 180:101644

3. Cairns NJ, Bigio EH, Mackenzie IRA, et al (2007) Neuropathologic diagnostic and nosologic criteria for frontotemporal lobar degeneration: consensus of the Consortium for Frontotemporal Lobar Degeneration. Acta Neuropathol (Berl) 114:5–22

4. Morris M, Maeda S, Vossel K, Mucke L (2011) The Many Faces of Tau. Neuron 70:410–426

5. Tracy T, Claiborn KC, Gan L (2019) Regulation of Tau Homeostasis and Toxicity by Acetylation. Adv Exp Med Biol 1184:47–55

6. Wesseling H, Mair W, Kumar M, et al (2020) Tau PTM Profiles Identify Patient Heterogeneity and Stages of Alzheimer's Disease. Cell 183:1699-1713.e13

7. de Calignon A, Fox LM, Pitstick R, Carlson GA, Bacskai BJ, Spires-Jones TL, Hyman BT (2010) Caspase activation precedes and leads to tangles. Nature 464:1201–1204

8. Ferrer I, Lopez-Gonzalez I, Carmona M, Arregui L, Dalfo E, Torrejon-Escribano B, Diehl R, Kovacs GG (2014) Glial and Neuronal Tau Pathology in Tauopathies: Characterization of Disease-Specific Phenotypes and Tau Pathology Progression. J Neuropathol Exp Neurol 73:17

9. Gamblin TC, Chen F, Zambrano A, et al (2003) Caspase cleavage of tau: linking amyloid and neurofibrillary tangles in Alzheimer's disease. Proc Natl Acad Sci U S A 100:10032–10037

10. Zhao Y, Tseng I-C, Heyser CJ, et al (2015) Appoptosin-Mediated Caspase Cleavage of Tau Contributes to Progressive Supranuclear Palsy Pathogenesis. Neuron 87:963–975

11. Gray DC, Mahrus S, Wells JA (2010) Activation of specific apoptotic caspases with an engineered small-molecule-activated protease. Cell 142:637–646

12. Hyman BT, Yuan J (2012) Apoptotic and non-apoptotic roles of caspases in neuronal physiology and pathophysiology. Nat Rev Neurosci 13:395–406

13. Albrecht S, Bourdeau M, Bennett D, Mufson EJ, Bhattacharjee M, LeBlanc AC (2007) Activation of caspase-6 in aging and mild cognitive impairment. Am J Pathol 170:1200–1209

14. Guo H, Albrecht S, Bourdeau M, Petzke T, Bergeron C, LeBlanc AC (2004) Active caspase-6 and caspase-6-cleaved tau in neuropil threads, neuritic plaques, and neurofibrillary tangles of Alzheimer's disease. Am J Pathol 165:523–531

15. Nikolaev A, McLaughlin T, O'Leary DDM, Tessier-Lavigne M (2009) APP binds DR6 to trigger axon pruning and neuron death via distinct caspases. Nature 457:981–989

16. Theofilas P, Ehrenberg AJ, Nguy A, et al (2018) Probing the correlation of neuronal loss, neurofibrillary tangles, and cell death markers across the Alzheimer's disease Braak stages: a quantitative study in humans. Neurobiol Aging 61:1–12

17. Dagbay KB, Hardy JA (2017) Multiple proteolytic events in caspase-6 self-activation impact conformations of discrete structural regions. Proc Natl Acad Sci 114:E7977–E7986

18. Graham RK, Ehrnhoefer DE, Hayden MR (2011) Caspase-6 and neurodegeneration. Trends Neurosci 34:646–656

19. Rissman RA, Poon WW, Blurton-Jones M, Oddo S, Torp R, Vitek MP, LaFerla FM, Rohn TT, Cotman CW (2004) Caspase-cleavage of tau is an early event in Alzheimer disease tangle pathology. J Clin Invest 114:121–130

20. Foveau B, Albrecht S, Bennett DA, Correa JA, LeBlanc AC (2016) Increased Caspase-6 activity in the human anterior olfactory nuclei of the olfactory bulb is associated with cognitive impairment. Acta Neuropathol Commun 4:127

21. Horowitz PM, Patterson KR, Guillozet-Bongaarts AL, Reynolds MR, Carroll CA, Weintraub ST, Bennett DA, Cryns VL, Berry RW, Binder LI (2004) Early N-terminal changes and caspase-6 cleavage of tau in Alzheimer's disease. J Neurosci Off J Soc Neurosci 24:7895–7902

22. Ramcharitar J, Albrecht S, Afonso VM, Kaushal V, Bennett DA, Leblanc AC (2013) Cerebrospinal fluid tau cleaved by caspase-6 reflects brain levels and cognition in aging and Alzheimer disease. J Neuropathol Exp Neurol 72:824–832

23. Eser RA, Ehrenberg AJ, Petersen C, et al (2018) Selective Vulnerability of Brainstem Nuclei in Distinct Tauopathies: A Postmortem Study. J Neuropathol Exp Neurol 77:149–161

24. Montine TJ, Phelps CH, Beach TG, et al (2012) National Institute on Aging-Alzheimer's Association guidelines for the neuropathologic assessment of Alzheimer's disease: a practical approach. Acta Neuropathol (Berl) 123:1–11

25. Mackenzie IRA, Neumann M, Bigio EH, et al (2010) Nomenclature and nosology for neuropathologic subtypes of frontotemporal lobar degeneration: an update. Acta Neuropathol (Berl) 119:1–4

26. Theofilas P, Wang C, Butler D, et al (2021) Caspase inhibition mitigates tau cleavage and neurotoxicity in iPSC-induced neurons with the V337M MAPT mutation. bioRxiv 2021.01.08.425912

27. Espinoza M, de Silva R, Dickson DW, Davies P (2008) Differential incorporation of tau isoforms in Alzheimer's disease. J Alzheimers Dis JAD 14:1–16

28. Goedert M, Jakes R, Crowther RA, Six J, Lübke U, Vandermeeren M, Cras P, Trojanowski JQ, Lee VM (1993) The abnormal phosphorylation of tau protein at Ser-202 in Alzheimer disease recapitulates phosphorylation during development. Proc Natl Acad Sci U S A 90:5066–5070

29. Jicha GA, Weaver C, Lane E, Vianna C, Kress Y, Rockwood J, Davies P (1999) cAMP-dependent protein kinase phosphorylations on tau in Alzheimer's disease. J Neurosci Off J Soc Neurosci 19:7486–7494

30. Zhou X-W, Li X, Bjorkdahl C, Sjogren MJ, Alafuzoff I, Soininen H, Grundke-Iqbal I, Iqbal K, Winblad B, Pei J-J (2006) Assessments of the accumulation severities of amyloid β-protein and hyperphosphorylated tau in the medial temporal cortex of control and Alzheimer's brains. Neurobiol Dis 22:657–668

31. Ehrenberg AJ, Morales DO, Piergies AMH, Li SH, Tejedor JS, Mladinov M, Mulder J, Grinberg LT (2020) A manual multiplex immunofluorescence method for investigating neurodegenerative diseases. J Neurosci Methods 108708

32. Coughlin DG, Dickson DW, Josephs KA, Litvan I (2021) Progressive Supranuclear Palsy and Corticobasal Degeneration. Adv Exp Med Biol 1281:151–176

33. Karikari TK, Pascoal TA, Ashton NJ, et al (2020) Blood phosphorylated tau 181 as a biomarker for Alzheimer's disease: a diagnostic performance and prediction modelling study using data from four prospective cohorts. Lancet Neurol 19:422–433

34. Cicognola C, Brinkmalm G, Wahlgren J, et al (2019) Novel tau fragments in cerebrospinal fluid: relation to tangle pathology and cognitive decline in Alzheimer's disease. Acta Neuropathol (Berl) 137:279–296

35. Sato C, Barthélemy NR, Mawuenyega KG, et al (2018) Tau kinetics in neurons and the human central nervous system. Neuron 97:1284-1298.e7

36. Chen Z, Mengel D, Keshavan A, et al (2019) Learnings about the complexity of extracellular tau aid development of a blood-based screen for Alzheimer's disease. Alzheimers Dement J Alzheimers Assoc 15:487–496

37. Chhatwal JP, Schultz AP, Dang Y, Ostaszewski B, Liu L, Yang H-S, Johnson KA, Sperling RA, Selkoe DJ (2020) Plasma N-terminal tau fragment levels predict future cognitive decline and neurodegeneration in healthy elderly individuals. Nat Commun 11:6024

38. Mengel D, Janelidze S, Glynn RJ, Liu W, Hansson O, Walsh DM (2020) Plasma NT1 Tau is a Specific and Early Marker of Alzheimer's Disease. Ann Neurol 88:878–892

39. Guillozet-Bongaarts AL, Glajch KE, Libson EG, Cahill ME, Bigio E, Berry RW, Binder LI (2007) Phosphorylation and cleavage of tau in non-AD tauopathies. Acta Neuropathol (Berl) 113:513–520

40. Canu N, Dus L, Barbato C, Ciotti MT, Brancolini C, Rinaldi AM, Novak M, Cattaneo A, Bradbury A, Calissano P (1998) Tau cleavage and dephosphorylation in cerebellar granule neurons undergoing apoptosis. J Neurosci Off J Soc Neurosci 18:7061–7074

41. Delobel P, Lavenir I, Fraser G, Ingram E, Holzer M, Ghetti B, Spillantini MG, Crowther RA, Goedert M (2008) Analysis of Tau Phosphorylation and Truncation in a Mouse Model of Human Tauopathy. Am J Pathol 172:123–131

42. LeBlanc A, Liu H, Goodyer C, Bergeron C, Hammond J (1999) Caspase-6 role in apoptosis of human neurons, amyloidogenesis, and Alzheimer's disease. J Biol Chem 274:23426–23436

43. Selznick LA, Holtzman DM, Han BH, Gökden M, Srinivasan AN, Johnson EM, Roth KA (1999) In situ immunodetection of neuronal caspase-3 activation in Alzheimer disease. J Neuropathol Exp Neurol 58:1020–1026

44. Grinberg LT, Heinsen H (2009) Argyrophilic grain disease: an update about a frequent cause of dementia. Dement Neuropsychol 3:2–7

45. Kovacs GG (2015) Invited review: Neuropathology of tauopathies: principles and practice. Neuropathol Appl Neurobiol 41:3–23

46. Karch CM, Kao AW, Karydas A, et al (2019) A Comprehensive Resource for Induced Pluripotent Stem Cells from Patients with Primary Tauopathies. Stem Cell Rep 13:939–955

Tables

Clinical diagnosis	Case	Sex	Age of death (years)	NIA-AA ABC scores
Alzheimer's disease	1	F	55-70	A3, B3, C3
	2	M	55-70	A3, B3, C3
	3	F	55-70	A3, B3, C3
Argyrophilic grain disease	1	F	75-90	A1, B2, C1
	2	F	75-90	A1, B1, C1
	3	M	75-90	A1, B1, C0
Corticobasal degeneration	1	M	60-75	A1, B1, C0
	2	F	60-75	A1, B1, C0
	3	M	60-75	A1, B1, C0
Pick's disease	1	M	60-70	A1, B0, C0
	2	F	60-70	A0, B1, C0
	3	M	60-70	A1, B1, C0
Progressive supranuclear palsy	1	F	65-70	A1, B1, C0
	2	M	65-70	A0, B1, C0
	3	M	65-70	A0, B0, C0
Control	1	M	75-90	A1, B1, C1
	2	F	75-90	A0, B1, C0

Table 1. Demographic, clinical, and neuropathological characteristics of the 17 cases included in the study. Abbreviations: NIA-AA, National Institute on Aging and Alzheimer's Association.

Variable	Middle frontal gyrus						Inferior temporal gyrus					
	AD	AGD	CBD	PiD	PSP	Control	AD	AGD	CBD	PiD	PSP	Control
n	3	3	3	3	3	2	3	3	3	2	3	2
Number of neurons (NeuN)	1290.33 (194.86)	1297.00 (221.47)	1267.33 (227.31)	1300.33 (519.59)	1191.67 (331.71)	863.00 (445.48)	1434.00 (484.36)	1305.00 (439.35)	1350.00 (97.32)	1082.00 (79.20)	1377.00 (25.24)	1148.50 (142.13)
Neuronal aCasp-6 (%)	8.74 (2.46)	0.00 (0.00)	0.09 (0.16)	4.15 (5.87)	0.22 (0.20)	0.00 (0.00)	8.79 (3.98)	0.34 (0.41)	0.33 (0.40)	1.26 (0.29)	0.12 (0.09)	0.00 (0.00)
Neuronal p-tau (%)	8.92 (5.83)	0.03 (0.06)	3.94 (2.33)	13.07 (7.56)	1.76 (0.88)	0.00 (0.00)	10.95 (3.42)	1.05 (1.07)	3.42 (3.04)	20.44 (17.19)	0.78 (0.80)	0.09 (0.01)
Neuronal D402 tr-tau (%)	8.67 (2.82)	0.00 (0.00)	0.00 (0.00)	0.97 (1.64)	0.54 (0.86)	0.00 (0.00)	7.08 (1.30)	0.32 (0.38)	0.03 (0.05)	0.98 (0.06)	0.12 (1.10)	0.04 (0.04)
Neuronal D13 tr-tau (%)	8.63 (5.62)	0.00 (0.00)	0.73 (0.47)	5.61 (4.40)	0.93 (0.62)	0.18 (0.26)	8.03 (2.69)	0.37 (0.34)	0.21 (0.20)	3.30 (2.05)	0.32 (0.49)	0.00 (0.00)
aCasp-6 + p-tau (%)	3.34 (1.64)	0.00 (0.00)	0.05 (0.08)	3.29 (4.47)	0.16 (0.20)	0.00 (0.00)	3.70 (0.48)	0.34 (0.41)	0.26 (0.39)	0.99 (0.66)	0.10 (0.11)	0.00 (0.00)
aCasp-6 + D402 tr-tau (%)	6.71 (2.67)	0.00 (0.00)	0.00 (0.00)	0.92 (1.60)	0.13 (0.22)	0.00 (0.00)	4.99 (1.57)	0.22 (0.23)	0.00 (0.00)	0.36 (0.23)	0.05 (0.04)	0.00 (0.00)
aCasp-6 + D13 tr-tau (%)	5.64 (2.71)	0.00 (0.00)	0.07 (0.12)	2.64 (3.33)	0.13 (0.22)	0.00 (0.00)	6.73 (2.57)	0.28 (0.31)	0.00 (0.00)	0.81 (0.78)	0.07 (0.13)	0.00 (0.00)
D402 tr-tau + p-tau (%)	2.31 (1.01)	0.00 (0.00)	0.00 (0.00)	0.80 (1.38)	0.54 (0.86)	0.00 (0.00)	2.59 (1.53)	0.24 (0.25)	0.03 (0.05)	0.80 (0.86)	0.07 (0.07)	0.00 (0.00)
D13 tr-tau + p-tau (%)	5.54 (4.37)	0.00 (0.00)	0.56 (0.40)	4.33 (3.57)	0.93 (0.62)	0.00 (0.00)	4.42 (0.33)	0.37 (0.34)	0.16 (0.22)	2.90 (1.62)	0.32 (0.49)	0.00 (0.00)
D402 tr-tau + D13 tr-tau (%)	4.32 (1.98)	0.00 (0.00)	0.00 (0.00)	0.86 (1.49)	0.41 (0.64)	0.00 (0.00)	4.25 (0.94)	0.21 (0.20)	0.03 (0.05)	0.36 (0.37)	0.02 (0.04)	0.00 (0.00)
aCasp-6 + D402 tr-tau + p-tau (%)	2.24 (1.03)	0.00 (0.00)	0.00 (0.00)	0.76 (1.32)	0.13 (0.22)	0.00 (0.00)	1.97 (1.18)	0.22 (0.23)	0.00 (0.00)	0.23 (0.05)	0.05 (0.04)	0.00 (0.00)
aCasp-6 + mAbD13 + p-tau (%)	2.99 (1.84)	0.00 (0.00)	0.05 (0.08)	2.42 (2.96)	0.13 (0.22)	0.00 (0.00)	3.37 (0.19)	0.28 (0.31)	0.00 (0.00)	0.73 (0.90)	0.07 (0.13)	0.00 (0.00)
aCasp-6 + D402 tr-tau + D13 (%)	4.27 (1.88)	0.00 (0.00)	0.00 (0.00)	0.83 (1.43)	0.13 (0.22)	0.00 (0.00)	4.06 (1.05)	0.21 (0.20)	0.00 (0.00)	0.14 (0.06)	0.02 (0.04)	0.00 (0.00)
mAbsD402 + D13 + p-tau (%)	2.03 (1.27)	0.00 (0.00)	0.00 (0.00)	0.73 (1.27)	0.41 (0.64)	0.00 (0.00)	2.03 (1.42)	0.21 (0.20)	0.03 (0.05)	0.22 (0.18)	0.02 (0.04)	0.00 (0.00)
aCasp-6 + D402 tr-tau + D13 + p-tau (%)	1.97 (1.17)	0.00 (0.00)	0.00 (0.00)	0.70 (1.21)	0.13 (0.22)	0.00 (0.00)	1.89 (1.21)	0.21 (0.20)	0.00 (0.00)	0.05 (0.07)	0.02 (0.04)	0.00 (0.00)

Table 2. Mean (SD) percent of neurons positive for the active caspase-6, D402 truncated tau, D13 truncated tau, phosphorylated tau, individually and by each combination of co-occurring markers. All cases showed neuronal p-tau positivity, as expected. Only AD cases showed neuronal caspase-6 positivity. AD and PiD cases showed the highest percentage of neurons positive for mAbsD402 and D13. Numbers for individual markers include neurons with more than one marker. Abbreviations: aCasp-6, active caspase-6; AD, Alzheimer's disease; AGD, argyrophilic grain disease; CBD, corticobasal degeneration; PiD, Pick's disease; PSP, progressive supranuclear palsy; p-tau, phosphorylated tau.

Figure Legends

Figure 1. Neuronal marker positivity from the middle frontal and inferior temporal gyrus of human postmortem brains with common tauopathies. Low and high magnification images were obtained using multiplex immunofluorescence staining of neurons (NeuN, blue), active caspase-6 (aCasp-6, orange), neoepitope mAbs of caspase-6-cleaved tau sites (D402 and D13, green and cyan, respectively), and phosphorylated tau (p-tau, magenta). AD (A) showed the most robust positivity for all markers than the other tauopathies (B-E), while no positivity was observed in controls. Abbreviations: AD, Alzheimer's disease (A); PiD, Pick's disease (B); CBD, corticobasal degeneration (C); PSP progressive supranuclear palsy (D); AGD, argyrophilic grain disease. Scale bars: 50 µm.

Figure 2. Multiplex immunofluorescence imaging showing colocalization of phospho-tau (Ser202, magenta), active caspase-6 (aCasp-6, orange), and neoepitope mAbs of caspase-6-cleaved tau sites (D402 and D13, green and cyan, respectively) in astroglial cells from human postmortem brains with CBD (A) and PSP (B). PSP (B) showed the greatest positivity for all markers compared to CBD (A). Abbreviations: CBD, corticobasal degeneration (A); PSP progressive supranuclear palsy (B). Scale bars: 50 µm.

Figure 3. Schematic of the semi-automated cell counting approach. First, single-channel images were stacked (Step one) followed by manual placement of counters on positive cells using FIJI's built-in counting tool (Step two). Next, counter coordinate data was extracted from FIJI files (Step three). The number and type of co-occurring markers were determined by searching for coordinates present within a two-pixel radius of each other using a Python script (Step four). Abbreviations: aCasp-6, active caspase-6; p-tau, phosphorylated tau.

Figure 4. Heatmap illustrating the mean proportion of neurons in the middle frontal and inferior temporal gyrus with antibody positivity for active caspase-6 (aCasp-6), mAbD402, mAbD13, phosphorylated tau (p-tau Ser202). AD, CBD, PiD, and PSP cases showed strong p-tau positivity in neurons, as expected. AD brains demonstrated the highest neuronal positivity for aCasp-6, mAbD402, and mAbD13, while PiD showed moderate positivity for these markers. CBD showed minimal positivity for mAbD13. AGD, CBD, showed minor positivity for aCasp-6, D402, and D13. No antibody positivity was present in controls. Abbreviations: AD, Alzheimer's disease; AGD, argyrophilic grain disease; CBD, corticobasal degeneration; PiD, Pick's disease; PSP, progressive supranuclear palsy. Rows represent cases with tauopathies, controls, and a list of antibodies included in the analysis. Columns represent the mean proportion of total neurons (color gradient) found positive for individual or multiple antibodies. The symbols +/- represent the presence (+, dark grey) or absence (-, light grey) of the antibody signal.

Figure 5. Venn diagrams illustrating the frequency of marker co-occurrence for AD and PiD, the two tauopathies with the highest marker positivity. Each colored disk represents mean numbers of positive neurons

for each antibody, including p-tau (yellow), mAbs D402 (cyan) and D13 (orange), and active Caspase-6 (grey) identified by multiplex immunofluorescence. Abbreviations: AD, Alzheimer's disease; PiD, Pick's disease; aCasp-6; active caspase-6; p-tau, phosphorylated tau.

Figure 6. Heatmap illustrating the mean proportion of phospho-tau positive glia in the middle frontal and inferior temporal gyrus of CBD and PSP brains, also found positive for active caspase-6 (aCasp-6), mAbD402, and mAbD13 antibodies. PSP and CBD were selected for analysis because they contain the highest astroglial pathology. PSP showed the greatest astroglial positivity for all markers, relative to CBD. Abbreviations: CBD, corticobasal degeneration; PSP, progressive supranuclear palsy. Rows represent cases with tauopathies, and a list of antibodies included in the analysis. Columns represent the mean proportion of total p-tau positive glia (color gradient), also found positive for individual or multiple antibodies. The symbols +/- represent the presence (+, dark grey) or absence (-, light grey) of the antibody signal.

Figure 1

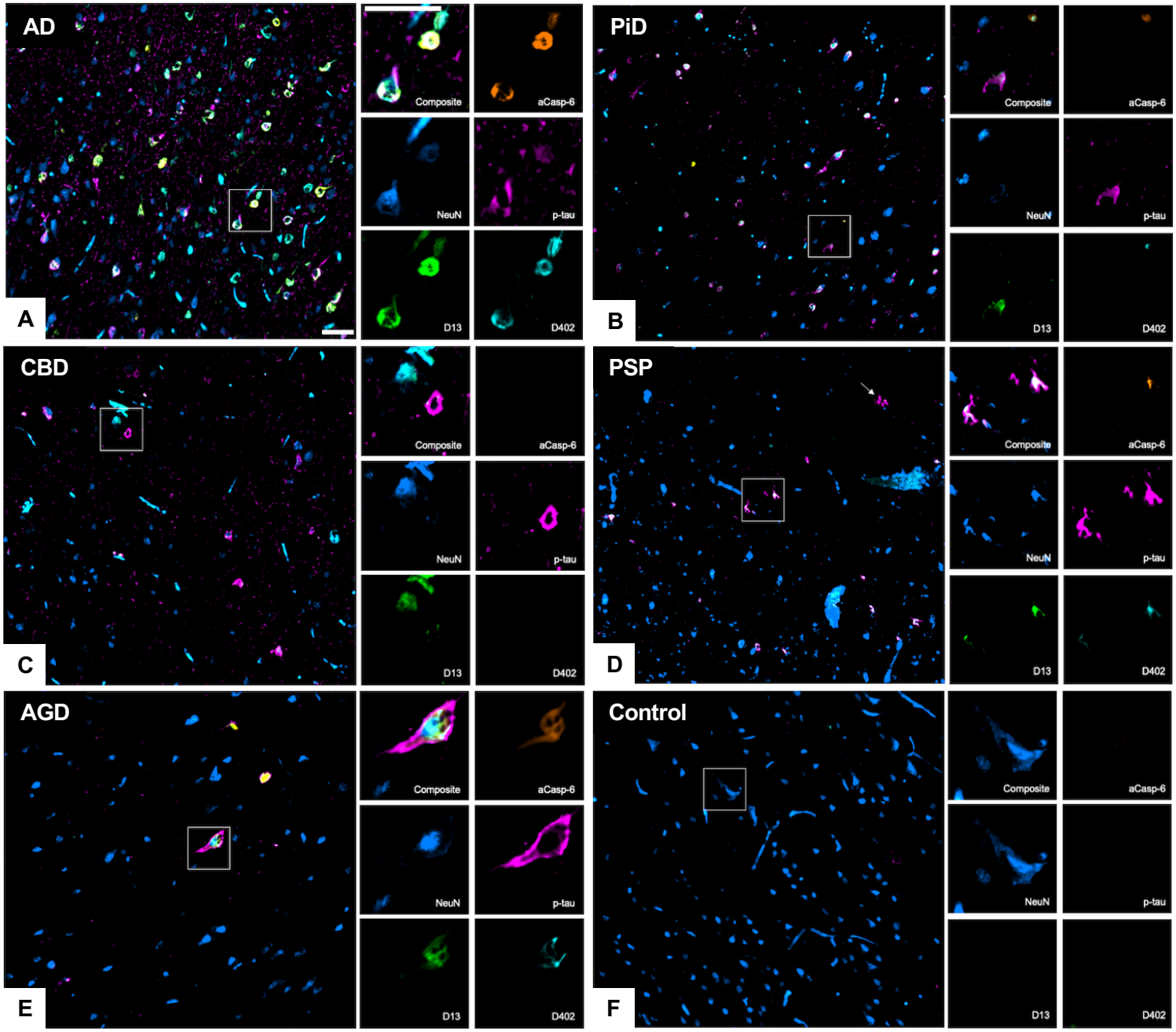

Figure 1. Neuronal marker positivity from the middle frontal and inferior temporal gyrus of human postmortem brains with common tauopathies. Low and high magnification images were obtained using multiplex immunofluorescence staining of neurons (NeuN, blue), active caspase-6 (aCasp-6, orange), neoepitope mAbs of caspase-6-cleaved tau sites (D402 and D13, green and cyan, respectively), and phosphorylated tau (p-tau, magenta). AD (A) showed the most robust positivity for all markers than the other tauopathies (B-E), while no positivity was observed in controls. Abbreviations: AD, Alzheimer's disease (A); PiD, Pick's disease (B); CBD, corticobasal degeneration (C); PSP progressive supranuclear palsy (D); AGD, argyrophilic grain disease. Scale bars: 50 μm.

Figure 2

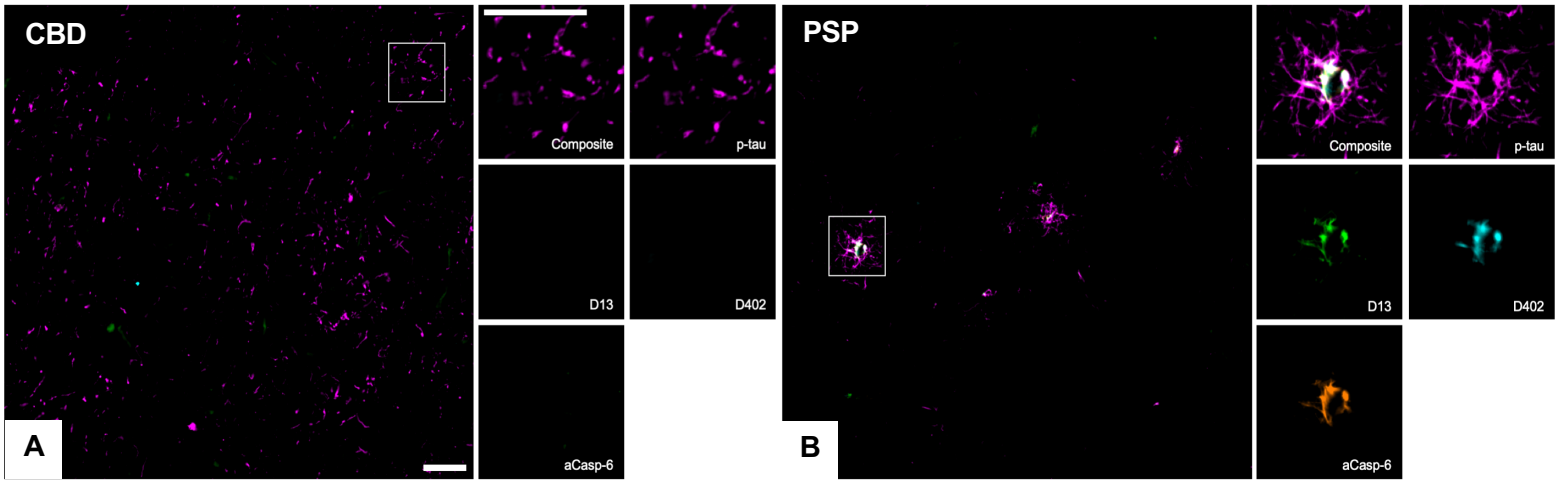

Figure 2. Multiplex immunofluorescence imaging showing colocalization of phospho-tau (Ser202, magenta), active caspase-6 (aCasp-6, orange), and neoepitope mAbs of caspase-6-cleaved tau sites (D402 and D13, green and cyan, respectively) in astroglial cells from human postmortem brains with CBD (A) and PSP (B). PSP (B) showed the greatest positivity for all markers compared to CBD (A). Abbreviations: CBD, corticobasal degeneration (A); PSP progressive supranuclear palsy (B). Scale bars: 50 µm.

Figure 3

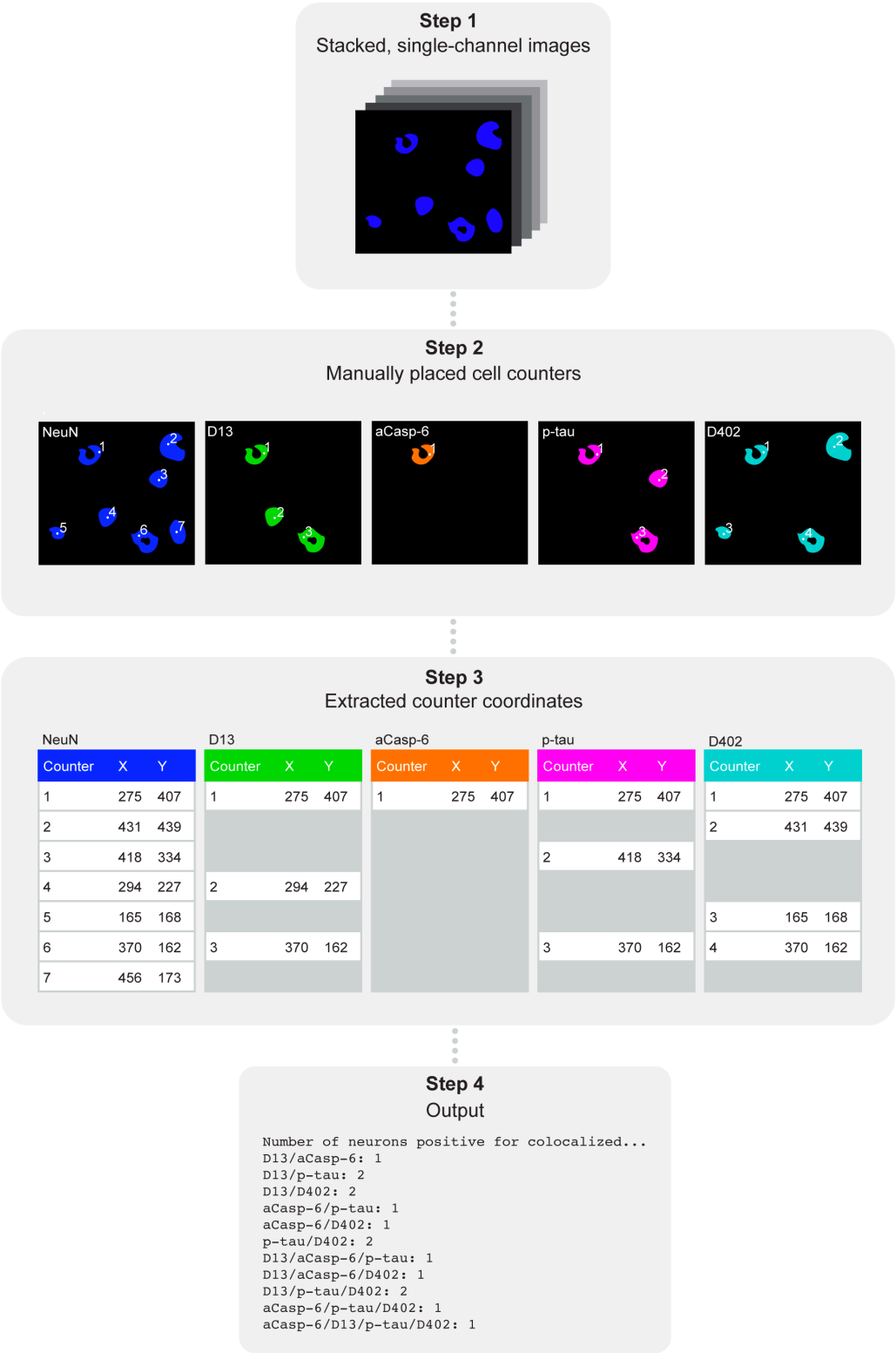

Figure 3. Schematic of the semi-automated cell counting approach. First, single-channel images were stacked (Step one) followed by manual placement of counters on positive cells using FIJI's built-in counting tool (Step two). Next, counter coordinate data was extracted from FIJI files (Step three). The number and type of co-occurring markers were determined by searching for coordinates present within a two-pixel radius of each other using a Python script (Step four). Abbreviations: aCasp-6, active caspase-6; p-tau, phosphorylated tau.

Figure 4

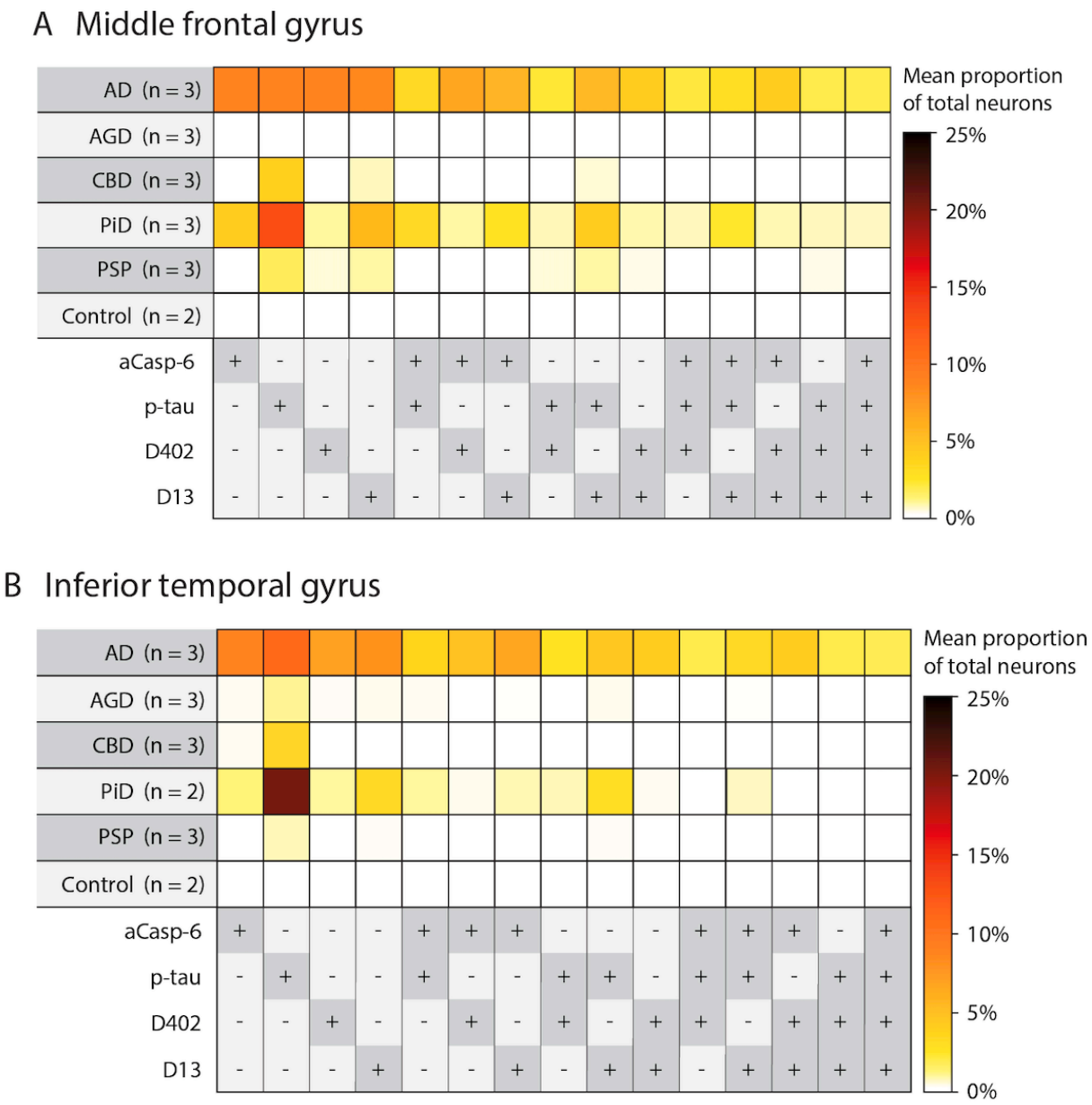

Figure 4. Heatmap illustrating the mean proportion of neurons in the middle frontal and inferior temporal gyrus with antibody positivity for active caspase-6 (aCasp-6), mAbD402, mAbD13, phosphorylated tau (p-tau Ser202). AD, CBD, PiD, and PSP cases showed strong p-tau positivity in neurons, as expected. AD brains demonstrated the highest neuronal positivity for aCasp-6, mAbD402, and mAbD13, while PiD showed moderate positivity for these markers. CBD showed minimal positivity for mAbD13. AGD, CBD, showed minor positivity for aCasp-6, D402, and D13. No antibody positivity was present in controls. Abbreviations: AD, Alzheimer's disease; AGD, argyrophilic grain disease; CBD, corticobasal degeneration; PiD, Pick's disease; PSP, progressive supranuclear palsy. Rows represent cases with tauopathies, controls, and a list of antibodies included in the analysis. Columns represent the mean proportion of total neurons (color gradient) found positive for individual or multiple antibodies. The symbols +/- represent the presence (+, dark grey) or absence (-, light grey) of the antibody signal.

Figure 5

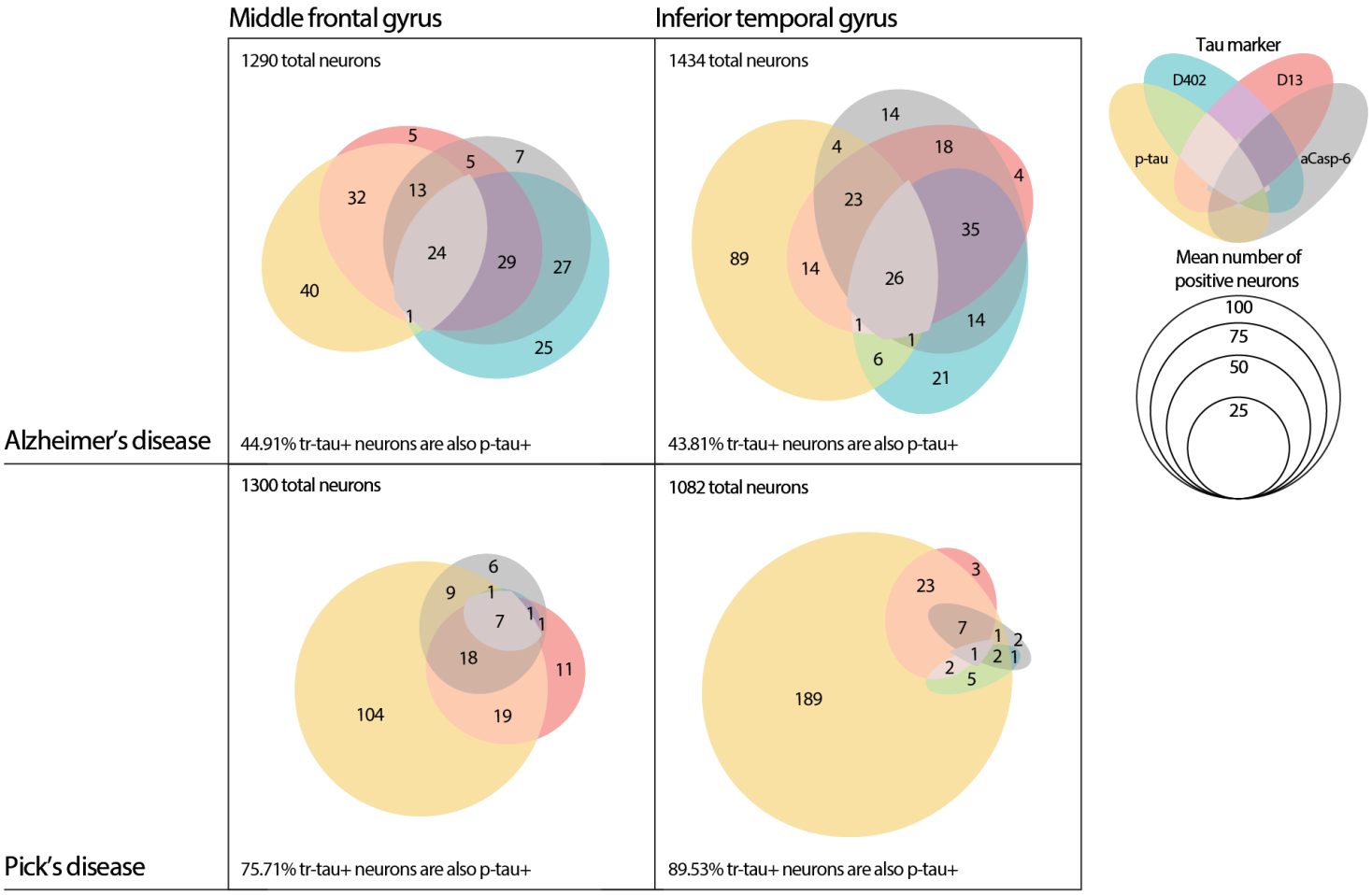

Figure 5. Venn diagrams illustrating the frequency of marker co-occurrence for AD and PiD, the two tauopathies with the highest marker positivity. Each colored disk represents mean numbers of positive neurons for each antibody, including p-tau (yellow), mAbs D402 (cyan) and D13 (orange), and active Caspase-6 (grey) identified by multiplex immunofluorescence. Abbreviations: AD, Alzheimer's disease; PiD, Pick's disease; aCasp-6; active caspase-6; p-tau, phosphorylated tau.

Figure 6

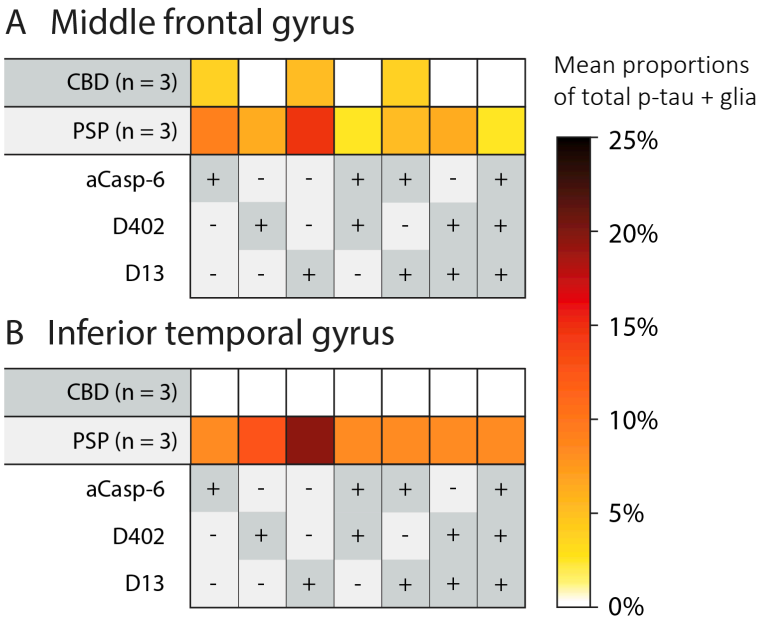

Figure 6. Heatmap illustrating the mean proportion of phospho-tau positive glia in the middle frontal and inferior temporal gyrus of CBD and PSP brains, also found positive for active caspase-6 (aCasp-6), mAbD402, and mAbD13 antibodies. PSP and CBD were selected for analysis because they contain the highest astroglial pathology. PSP showed the greatest astroglial positivity for all markers, relative to CBD. Abbreviations: CBD, corticobasal degeneration; PSP, progressive supranuclear palsy. Rows represent cases with tauopathies, and a list of antibodies included in the analysis. Columns represent the mean proportion of total p-tau positive glia (color gradient), also found positive for individual or multiple antibodies. The symbols +/- represent the presence (+, dark grey) or absence (-, light grey) of the antibody signal.